JOURNAL OF COMPUTATIONAL PHYSICS 42, 195–211 (1981)

Pseudo-unsteady Difference Schemes for Discontinuous Solutions of Steady-State, One-Dimensional Fluid Dynamics Problems

LAN CHIEH HUANG

Computing Center, Academia Sinica, Beijing, China

Received September 11, 1980; revised January 29, 1981

This paper presents two unsteady difference schemes for one-dimensional steady-state shock solutions starting from the pseudo-unsteady equations. The so-called explicit upwind scheme is actually an explicit forward-time, centered-space difference scheme with an appropriate artificial viscosity term, which depends on the directions of the characteristics. This scheme, considered as an iterative scheme, has good convergence properties, and leads to steady-state numerical shocks, each with at most one point of transition, regardless of the position of the shock with respect to the mesh. The mesh can be refined locally and computation continued locally to make the profile of the shock sharper. To increase the rate of convergence, the corresponding implicit scheme is presented. Results of numerical tests for a shock tube and a convergent–divergent nozzle are given.

1. INTRODUCTION

There are generally two types of finite difference methods for the solution of steady-state problems: the iterative methods and the unsteady methods. For some problems, fast convergent iterative schemes are available.But for many complicated problems, effective, or even just convergent, iterative schemes are very difficult to find. For these problems it is natural to follow the true physical process and solve the time-dependent problem, whose asymptotic solution is the desired steady-state solution. But as the entire time-dependent process is found, the amount of work involved can be considerable. So quite often some requirements are relaxed in the time-dependent process. For example, it is only necessary for the difference scheme to be consistent with the original equation in the steady state, and to reduce the amount of work, one can use unsteady equations with different physical meaning from the original one, or even use unsteady equations which have no true physical meaning at all, see, for example, [1–3].

Time-dependent difference methods for discontinuous solutions are divided into two categories: the shock-fitting methods and the pseudo-viscosity methods. With the former, one can obtain shocks with sharp profiles, but the programming can be very complicated. With the latter, one can capture shocks with one uniform difference scheme, but usually either smearing or oscillation occurs in the vicinity of the shocks.

0021 9991/81/070195-17$02.00/0

There are uniform schemes which give "sharp" shock profiles, for example, the Glimm scheme (see Chorin [4]), resulting in shock profiles with no point of transition, and the one-sided schemes of Engquist and Osher [5], yielding steady-state discontinuities with two points of transition. Also MacCormack *et al.* [6] used a uniform scheme for the solution of flow around an arbitrary blunt body, where a sharp profile shock was obtained. However, with the MacCormack scheme, it is necessary for the shock to be midway between two neighboring mesh points, otherwise oscillation will result. For steady-state shocks, smearing or oscillation of the numerical result is often caused by the steady-state difference equation itself and not by the unsteady method used to solve it. This has been observed by, for example, Crocco [1], and Roache [7, p. 161]. It is along this line of reasoning that the author presents difference schemes which yield "clear" steady-state shock profiles. A "clear" profile means a profile of numerical discontinuity with at most one point of transition, regardless of the position of the discontinuity with respect to the mesh. These schemes are presented with the intention of contributing to the whole effort of obtaining sharp shock profiles with uniform schemes.

The present author made a study in [8] of the rate of convergence of unsteady difference schemes considered as iterative schemes for steady-state problems, with a one-dimensional linear hyperbolic equation with constant coefficients. By fixing the mesh, the correspoonding matrices of the unsteady schemes were studied; the matrix properties determine the convergence. (In this paper convergence always means iterative convergence.) Several schemes commonly used for fluid dynamics problems were considered. Because these matrices are quite different in nature from those obtained from schemes for the numerical solution of second order elliptic equations and because their complete analysis is difficult, it is required, at least, that the schemes, considered as schemes for pure intial value problems, be stable.

A part of the results of [8] is that for a first order hyperbolic equation, the explicit upwind (upwind means a scheme which depends on the directions of the characteristics) scheme converges faster than the Lax–Wendroff scheme; and that the implicit upwind scheme converges very fast for large Courant numbers; it converges faster than the Crank–Nicholson scheme with the equivalent steady-state viscosity. In [8], the author also discussed unsteady schemes for steady-state discontinuous solutions of the nonlinear model equation. It was found that the upwind schemes yield steady-state discontinuous solutions with clear profiles.

This paper extends some of the results of [8] to the case of steady-state discontinuous solutions of one-dimensional fluid dynamics problems. The equations used are those which Denton [3] called the pseudo-unsteady equations. These equations have led to some very good results in the calculation of steady-state cascade flow through turbomachinery, see also [9]. After establishing some properties of the pseudo-unsteady equations, the explicit upwind scheme will be constructed and discussed. This scheme has good convergence properties and leads to steady-state numerical shocks with one point of transition. It lacks certain other important properties; for example, in contrast with the Engquist and Osher schemes, it is not monotone. But given suitable initial values, it will lead to the physically relevant

solutions, as does the Lax–Wendroff scheme. Numerical results, which are given after a brief statement of the boundary conditions, verify this. The corresponding implicit scheme will also be discussed; its simplification follows that of Beam and Warming [10], but the scheme is "full" implicit and not of the Crank–Nicholson type. With the implicit scheme, the same results as those with the explicit scheme are obtained, but the convergence is faster.

2. The Pseudo-Unsteady Equations

Let us consider the following one-dimensional pseudo-unsteady equations:

$$\frac{\partial(\rho S)}{\partial t} + \frac{\partial(\rho u S)}{\partial x} = 0, \tag{2.1}$$

$$\frac{\partial(\rho u S)}{\partial t} + \frac{\partial(\rho u^2 S)}{\partial x} + S\frac{\partial p}{\partial x} = 0, \tag{2.2}$$

$$h + \frac{u^2}{2} = \text{const.} = H, \tag{2.3}$$

where S is the cross-sectional area of the one-dimensional flow duct, u, ρ, p, h are, respectively, the velocity, density, pressure, and enthalpy of the gas. (2.1), (2.2), (2.3) represent, respectively, the unsteady conservation of mass, unsteady conservation of momentum, and the steady-state relation of constant total enthalpy. From the equation of state, we have

$$p = \rho RT = \rho\frac{\gamma - 1}{\gamma}\left(H - \frac{u^2}{2}\right), \tag{2.4}$$

where R is the gas constant and γ is the specific heat ratio. So we have simply a system of two equations for two unknowns, ρ and u, which is simpler than the system of three true unsteady equations for three unknowns.

It is easily seen that the steady-state shock conditions for the pseudo-unsteady equations are the true steady-state shock conditions.

(2.1), (2.2) can be written as

$$\frac{\partial}{\partial t}\begin{pmatrix}\rho\\ u\end{pmatrix} + \begin{pmatrix}u & \rho\\ a^2/\gamma\rho & u/\gamma\end{pmatrix}\frac{\partial}{\partial x}\begin{pmatrix}\rho\\ u\end{pmatrix} = \cdots,$$

where the right hand side does not involve partial derivatives of the unknowns. Denote the above matrix by M, its eigenvalues are

$$\lambda_{\pm} = \frac{(\gamma + 1)u \pm s}{2\gamma}, \tag{2.5}$$

where $s = ((\gamma+1)^2 u^2 - 4\gamma(u^2 - a^2))^{1/2}$, and a is the sound speed $(=(\gamma RT)^{1/2})$. Because s is real and $\neq 0$, $\lambda_\pm$ are two distinct real numbers, so the system is hyperbolic, and $dx/dt = \lambda_\pm$ are the characteristic directions. When $u < a$, one is positive, one negative; when $u = a$, one is positive, one zero; and when $u > a$, both are positive.

Following the derivation for the matrix properties for the unsteady fluid dynamic equations, see Steger [11] and Warming *et al.* [12], we arrive at similar matrix properties for our pseudo-unsteady equations. First of all, we obtain a non-singular matrix T such that

$$M = T\Lambda T^{-1}, \qquad \Lambda = \begin{pmatrix} \lambda_+ & 0 \\ 0 & \lambda_- \end{pmatrix}, \tag{2.6a}$$

with

$$T = \begin{pmatrix} 1 & 1 \\ \dfrac{(1-\gamma)u + s}{2\gamma\rho} & \dfrac{(1-\gamma)u - s}{2\gamma\rho} \end{pmatrix}. \tag{2.6b}$$

Now write (2.1), (2.2) as

$$\frac{\partial U}{\partial t} + \frac{\partial F}{\partial x} + S\frac{\partial G}{\partial x} = 0, \tag{2.7a}$$

where

$$U = \begin{pmatrix} \rho S \\ \rho u S \end{pmatrix}, \qquad F = \begin{pmatrix} \rho u S \\ \rho u^2 S \end{pmatrix}, \qquad G = \begin{pmatrix} 0 \\ \dfrac{\gamma-1}{\gamma}\rho\left(H - \dfrac{u^2}{2}\right) \end{pmatrix}. \tag{2.7b}$$

Let

$$A = \frac{\partial F}{\partial U} = \begin{pmatrix} 0 & 1 \\ -u^2 & 2u \end{pmatrix}, \qquad SB = S\frac{\partial G}{\partial U} = \begin{pmatrix} 0 & 0 \\ \dfrac{a^2 + (\gamma-1)u^2}{\gamma} & -\dfrac{\gamma-1}{\gamma}u \end{pmatrix}; \tag{2.8}$$

we can easily see that

$$F = AU, \qquad SG = SBU. \tag{2.9}$$

Now let

$$C = A + SB; \tag{2.10}$$

we can obtain

$$C = \tilde{T}M\tilde{T}^{-1}, \tag{2.11a}$$

where

$$\tilde{T} = \begin{pmatrix} 1 & 0 \\ u & \rho \end{pmatrix}. \tag{2.11b}$$

From (2.6), (2.11), we get non-singular matrix $Q = \tilde{T}T$ such that

$$C = Q\Lambda Q^{-1}. \tag{2.12}$$

These results will be used in the following sections.

3. The Explicit Upwind Scheme

For the simplest linear hyperbolic equation

$$\frac{\partial u}{\partial t} + \frac{\partial u}{\partial x} = 0, \tag{3.1}$$

the explicit upwind scheme is

$$u_j^{n+1} = ru_{j-1}^n + (1-r)\,u_j^n, \tag{3.2}$$

where $r = \Delta t/\Delta x$. Suppose we solve the equation on $0 \leqslant x \leqslant 1$, $t \geqslant 0$, with the following boundary and initial conditions:

$$u(0, t) = 0, \tag{3.3a}$$

$$u(x, 0) = u_0(x), \tag{3.3b}$$

with $u_0(x)$ given. Divide the x interval into J equal parts, so $J\Delta x = 1$, then we may write

$$U^{n+1} = C_\Delta U^n, \tag{3.4}$$

where U^n is the vector with components u_j^n, $j = 1, 2, \ldots, J$, C_Δ is the J dimensional tridiagonal matrix $(r, 1-r, 0)$, where we let J be fixed. Its eigenvalues are obviously

$$a_E = 1 - r. \tag{3.5}$$

For the Lax–Wendroff scheme with the additional boundary condition $u(1, t) = 0$, $C_\Delta = (r/2 + r^2/2,\ 1 - r^2,\ -r/2 + r^2/2)$, with dimension $J - 1$. Using

$$\det(a, b, c) = 0 \Leftrightarrow b = 2(ac)^{1/2} \cos\frac{j\pi}{J}, \qquad j = 1, 2, \ldots, J-1, \tag{3.6}$$

see [13], we obtain for the Lax–Wendroff scheme

$$\alpha_{LW} = 1 - r^2 + ir(1 - r^2)^{1/2} \cos \frac{j\pi}{J}, \qquad j = 1, 2, \ldots, J - 1. \tag{3.7}$$

For large J, $|\alpha_{LW}|_{\max} \sim (1 - r^2)^{1/2}$, so for $0 < r < 1$, $|\alpha_E| < |\alpha_{LW}|_{\max}$. We see that the asymptotic rate of convergence for the explicit upwind scheme is higher than that for the Lax–Wendroff scheme. For further discussion and for comparison with other schemes, see [8], where also the behavior of $\|C_\Delta^n\|_1$ is studied, especially for other boundary conditions.

For the nonlinear model equation

$$\frac{\partial u}{\partial t} + \frac{\partial f}{\partial x} = 0, \qquad f = \frac{u^2}{2}, \tag{3.8}$$

consider the following upwind scheme:

$$u_j^{n+1} = u_j^n - q(f_{j+1/2}^n - f_{j-1/2}^n), \tag{3.9a}$$

where

$$\begin{aligned} f_{j+1/2}^n &= (u_{j+1}^n)^2/2, && \text{if } u_{j+1/2}^n < 0, \\ &= ((u_{j+1}^n)^2/2 + (u_j^n)/2)/2, && \text{if } u_{j+1/2}^n = 0, \\ &= (u_j^n)^2/2, && \text{if } u_{j+1/2}^n > 0, \end{aligned} \tag{3.9b}$$

$u_{j+1/2}^n = (u_{j+1}^n + u_j^n)/2$ and $q = \Delta t/\Delta x$. If $u_{j+1/2}^n < 0$ always (or > 0 always), then we have the usual one-sided scheme. Note, for smooth solutions, $\varepsilon_j^n = u_j^n - u_j$ satisfies the linear equation (3.2), with $r = uq$, so the convergence of the scheme is as above. Also the corresponding steady-state equation of (3.9) admits steady-state discontinuous solutions with clear profiles, and numerical experiments show that (3.9) leads indeed to such solutions, see [8].

(3.9) can be written as

$$\begin{aligned} u_j^{n+1} = u_j^n - \frac{\Delta t}{2\Delta x}(f_{j+1}^n - f_{j-1}^n) + \mu \frac{\Delta t}{\Delta x^2}[&\operatorname{sign}(u_{j+1/2}^n)(f_{j+1}^n - f_j^n) \\ &- \operatorname{sign}(u_{j-1/2}^n)(f_j^n - f_{j-1}^n)], \end{aligned} \tag{3.10}$$

where $\mu \Delta t/\Delta x^2 = \Delta t/2\Delta x$. For pseudo-unsteady equations (2.7), we wish to construct a corresponding scheme. But what should the $\operatorname{sign}(u) = \operatorname{sign}(df/du)$ for one equation be for a system of equations? It should be something like sign C, where $C = \partial F/\partial U + S(\partial G/\partial U) = A + SB$. Considering (2.12), we define sign C as:

$$\operatorname{sign} C = Q(\operatorname{sign} \Lambda) Q^{-1} = Q \begin{pmatrix} \operatorname{sign}(\lambda_+) & 0 \\ 0 & \operatorname{sign}(\lambda_-) \end{pmatrix} Q^{-1}.$$

Using (2.6), (2.11), we get

$$\begin{aligned}\operatorname{sign} C &= \begin{pmatrix} 1 & 0 \\ 0 & 1 \end{pmatrix}, && \text{if} \quad \lambda_+ > 0, \lambda_- > 0, \\ &= \begin{pmatrix} 0 & \gamma/(\gamma+1)u \\ 0 & 1 \end{pmatrix}, && \text{if} \quad \lambda_- > 0, \lambda_+ = 0, \\ &= \frac{1}{s}\begin{pmatrix} -(\gamma+1)u & 2\gamma \\ 2(a^2-u^2) & (\gamma+1)u \end{pmatrix}, && \text{if} \quad \lambda_- > 0, \lambda_+ < 0. \end{aligned} \tag{3.11}$$

Corresponding to (3.10), we have now the following scheme:

$$\begin{aligned} U_j^{n+1} = U_j^n &- \frac{q}{2}\left[(F_{j+1}^n - F_{j-1}^n) + S_{j+1/2}(G_{j+1}^n - G_j^n) + S_{j-1/2}(G_j^n - G_{j-1}^n)\right] \\ &+ \frac{q}{2}\{\operatorname{sign} C_{j+1/2}^n\left[(F_{j+1}^n - F_j^n) + S_{j+1/2}(G_{j+1}^n - G_j^n)\right] \\ &- \operatorname{sign} C_{j-1/2}^n\left[(F_j^n - F_{j-1}^n) + S_{j-1/2}(G_j^n - G_{j-1}^n)\right]\}. \end{aligned} \tag{3.12}$$

Let $E_j^n = U_j^n - U_j$, for smooth solutions, E_j^n satisfies

$$E_j^{n+1} = E_j^n - \frac{q}{2}C(E_{j+1}^n - E_{j-1}^n) + \frac{q}{2}(\operatorname{sign} C)\, C(E_{j+1}^n - 2E_j^n + E_{j-1}^n),$$

where higher order small quantities and lower order differences have been neglected and the coefficients have been taken locally as constants. Let $V = Q^{-1}E$; then

$$V_j^{n+1} = V_j^n - \frac{q}{2}\left[\Lambda(V_{j+1}^n - V_{j-1}^n) + (\operatorname{sign}\Lambda)\,\Lambda(V_{j+1}^n - 2V_j^n + V_{j-1}^n)\right].$$

Note $(\operatorname{sign}\Lambda)\Lambda = \begin{pmatrix} |\lambda_+| & 0 \\ 0 & |\lambda_-| \end{pmatrix}$, so we have two separate upwind difference equations. As an iterative scheme, with appropriate boundary conditions, convergence is as above. We will not go into the problem of general boundary conditions here. The first variational equation of (3.12) is of the same form as that of E_j^n, so stability of (3.12) as an evolutionary scheme for pure initial value problems, is ensured if $\lambda_+ q \leqslant 1$.

The corresponding steady-state scheme of (3.12) is

$$\begin{aligned} &(I - \operatorname{sign} C_{j+1/2})\left[(F_{j+1} - F_j) + S_{j+1/2}(G_{j+1} - G_j)\right] \\ &\quad + (I + \operatorname{sign} C_{j-1/2})\left[(F_j - F_{j-1}) + S_{j-1/2}(G_j - G_{j-1})\right] = 0. \end{aligned} \tag{3.13}$$

Let the flow be from left to right, and M be a point as shown in Fig. 1, with $u_{j_M-1/2}$ supersonic and $u_{j_M+1/2}$ subsonic. Suppose

$$(F_j - F_{j-1}) + S_{j-1/2}(G_j - G_{j-1}) = 0, \qquad j-1, j \neq j_M, \tag{3.14a}$$

$$(F_R - F_M) + S_{MR}(G_R - G_M) + (F_M - L_L) + S_{LM}(G_M - G_L) = 0 \tag{3.14b}$$

hold (S_{MR} denote the value of S at the midpoint between M and R, S_{LM} likewise). We will show that (3.13) admits discontinuous solutions with clear profiles. When point M is not involved, (3.13) holds because of (3.14a). When M is involved, we examine the three sets of points, (I, L, M), (L, M, R), and (M, R, E) in turn to see what conditions other than (3.14) are necessary for (3.13) to be valid. For (I, L, M), we have sign $C_{j+1/2} = \text{sign } C_{j-1/2} = I$, (3.13) becomes $2[F_L - F_I + S_{IL}(G_L - G_I)] = 0$, which holds due to (3.14a). For (L, M, R), sign $C_{j-1/2} = I$, (3.13) becomes

$$(I - \text{sign } C_{MR})[F_R - F_M + S_{MR}(G_R - G_M)] + 2[F_M - F_L + S_{LM}(G_M - G_L)] = 0.$$

Using (3.14b), we arrive at

$$(I + \text{sign } C_{MR})[F_R - F_M + S_{MR}(G_R - G_M)] = 0. \tag{3.15}$$

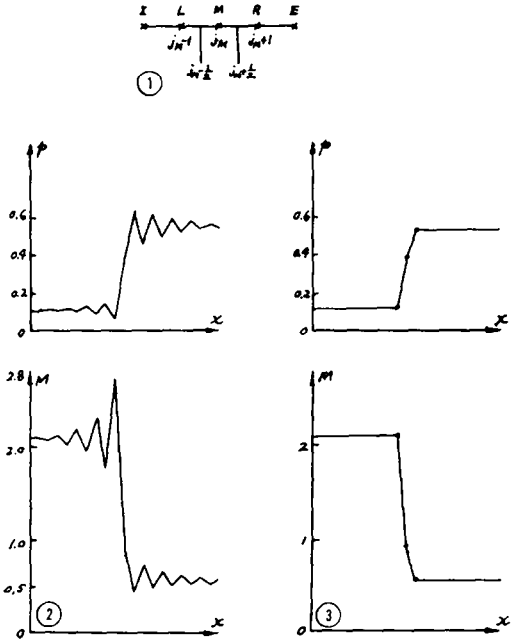

FIGS. 1–3. (1) Point of transition. (2) Shock tube MacCormack scheme ($n = 256$, $\varepsilon = 0.5 \times 10^{-3}$). (3) Shock tube explicit upwind scheme ($n = 208$, $\varepsilon = 0.6 \times 10^{-5}$).

Noting that

$$\det(I + \operatorname{sign} C_{MR}) = 0,$$

we see that (3.15) represents just one relation which we may write as

$$\begin{aligned}&|I - (\gamma + 1)\, u + s|_{MR}\, [(\rho uS)_R - (\rho uS)_M] \\ &\quad + 2\gamma|(\rho u^2 S)_R - (\rho u^2 S)_M + S_{MR}(p_R - p_M)| = 0. \end{aligned} \tag{3.16}$$

It is easily seen that for (M, R, E), we also arrive at (3.16). Hence (3.14) and only one more relation (3.16) imply (3.13).

Now, for constant S, we see that (3.14) are $2(J-1)$ equations not involving point M, with two boundary conditions (one on the left and one on the right), they determine $2J$ unknowns (on J points: $0, 1, \ldots, j_M - 1, j_M + 1, \ldots, J$). A steady progressing shock in a shock tube (with consant states on both sides of the shock) will satisfy these equations exactly. (3.16) is one relation for the two unknowns at M, the actual values of the unknowns can vary, allowing the position of the shock to vary with respect to the mesh.

From the qualitative analysis above, we see that steady-state scheme (3.13) of (3.12) admits numerical discontinuous solutions with clear profiles; hence with (3.12), we can hope to arrive at such steady-state solutions. Numerical results presented below demonstrate that indeed we do obtain such solutions.

We note here that in general

$$(\rho uS)_M \neq (\rho uS)_L = (\rho uS)_R = m_0, \tag{3.17}$$

so values at M do not have any real physical meaning. M is a mathematical transition point, and we can use (3.17) to identify it.

4. Boundary Conditions

From this section on, all quantities will be dimensionless, the reference parameters are length L, state T^0, p^0, $\rho^0 = p^0/RT^0$, and $a^0 = (\gamma RT^0)^{1/2}$. (2.7), (2.3) will be unchanged, but

$$p = \rho T = \rho(\gamma - 1)(H - u^2/2), \tag{4.1}$$

where following [14], we take $H = 1$.

At the inlet, if the flow is subsonic, one boundary condition is given, say,

$$p_{si} = 1, \tag{4.2}$$

where subscript s denotes stagnation state and i the inlet. At the outlet, if the flow is also subsonic, one boundary condition is given, say,

$$p_e = p_{e0}, \tag{4.3}$$

where subscript e denotes the exit and p_{e0} is a given constant; but if it is supersonic, then no boundary conditions need to be given.

For our scheme, additional boundary conditions are needed. We may lengthen the duct and take $\partial/\partial x$ of some unknown equal to zero, as is often done in the literature. Or better, we can use (3.14a) at the boundaries, ρS and ρuS at the boundaries may be obtained from (3.12), which becomes one-sided. If the flow is subsonic, divide and get u, calculate T, then from (4.2) or (4.3) we get ρ. If the outflow is supersonic, we leave the ρS and ρuS as they stand. We will refer to this as the "scheme" boundary condition.

5. Numerical Results

The first example is taken from [15, p. 343], the flow field in a shock tube. The coordinate axis is taken such that the flow is from left to right and the steady-state shock speed is zero. For the sake of simplicity, fixed boundary conditions were considered, $J = 40$, and initial condition such that the values on the left 10 points and the right 10 points were the same as those on the respective boundaries, values at intermediate points were linear interpolations of these. Both the MacCormack scheme and the upwind scheme (3.12) were tested with $q = 0.5$ (the stability condition being $q = 0.73$); both gave steady-state solutions. It is difficult to determine the shock position, but this is not important. What is important is that the upwind scheme led to a steady-state discontinuous solution with one point of transition, while the MacCormack scheme led to results with oscillation, also its convergence was slower, see Figs. 2, 3.

The second example is taken from [14], the flow field in a convergent–divergent nozzle. The length of the nozzle is 10, cross-sectional area at the inlet and outlet is 1.5 and at the throat 1, in between it varies as the sine curve. When $p_e > 0.8805$ the flow is all subsonic; when $p_e < 0.1602$, the flow changes smoothly from subsonic at the inlet to transonic at the throat to supersonic at the outlet; there are no shocks. When $0.1602 < p_e < 0.8805$, there is a shock to the right of the throat, the flow field to the left of the shock is as above, but changes from supersonic to subsonic through the shock. The critical mass flow is 0.9150.

At the start of the numerical experiment, the scheme was not entirely as (3.12), $S_{j+1/2}(G^n_{j+1} - G^n_j) + S_{j-1/2}(G^n_j - G^n_{j-1})$ on the right hand side was one term $S_j(G^n_{j+1} - G^n_{j-1})$; also in $C_{j+1/2}$,

$$u_{j+1/2} = \frac{(\rho uS)_j + (\rho uS)_{j+1}}{(\rho S)_j + (\rho S)_{j+1}}. \tag{5.1}$$

Such a scheme was tested for two cases, $p_e = 0.16$ and 0.70, with $\Delta x = 0.5$, $J = 40$. The initial condition was as example one. For all boundary conditions considered, the numerical result tended to the steady-state solution until $\|U^{n+1} - U^n\| = \max_j(|U^{n+1}_{1_j} - U^n_{1_j}| + |U^{n+1}_{2_j} - U^n_{2_j}|) \leqslant \varepsilon \sim 10^{-3}$, then it started to drift and the mass

flow started to decrease, so that the steady-state solution was never reached. After changing to (3.12), where the first order differences were consistent with those in the second order difference terms, the steady-state solutions were obtained, the results are shown in Figs. 4 and 5 (only results near transonic flow and the shock wave are shown, the rest coincide with the exact solution on the graph).

The numerical results with fixed boundary conditions are quite good, and the convergence faster. But in actual computation we cannot give such boundary conditions, so we will not discuss this type of boundary conditions in detail.

It seems that for discontinuous solutions, lengthening the duct (here $\partial\hat{c}/\partial x = 0$ and scheme boundary conditions are the same) causes large errors in the numerical results; the numerical steady-state mass flow (at all points other than M) is $m_0 = 0.9109$, which is within 0.45% of the exact mass flow. This affects the flow field more apparently at the throat, as transonic flow is very sensitive to any change in mass flow. But by halving the mesh size, $\Delta x = 0.25$, $J = 80$, the numerical steady-state mass flow increased to about 0.914.

In order to save computing time, scheme boundary conditions were considered. The numerical results for $p_e = 0.70$ with $\Delta x = 0.5$, $J = 20$, and the initial condition being simply linear interpolation of exact boundary values, are shown in Fig. 5. We see that the results are quite good, and the number of iterations has decreased for the same error tolerance, as there are now also less mesh points.

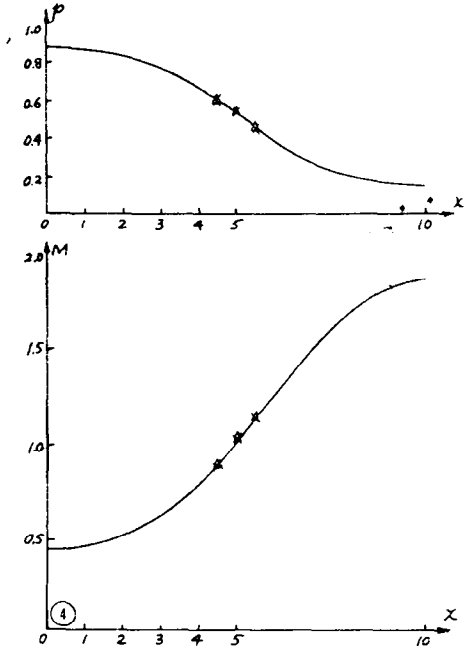

FIG. 4. Nozzle $p_e = 0.16$. (—) Exact solution. (Δ) Fixed boundary condition, $\Delta x = 0.5$, $q = 0.5$, $n = 320$, $\varepsilon = 0.9 \times 10^{-4}$; $n = 560$, $\varepsilon = 0.1 \times 10^{-6}$. (×) Lengthen the duct b.c., $\Delta x = 0.5$, $q = 0.5$, $n = 592$, $\varepsilon = 0.9 \times 10^{-4}$; $n = 1408$, $\varepsilon = 0.6 \times 10^{-7}$ ($m_0 = 0.9157$).

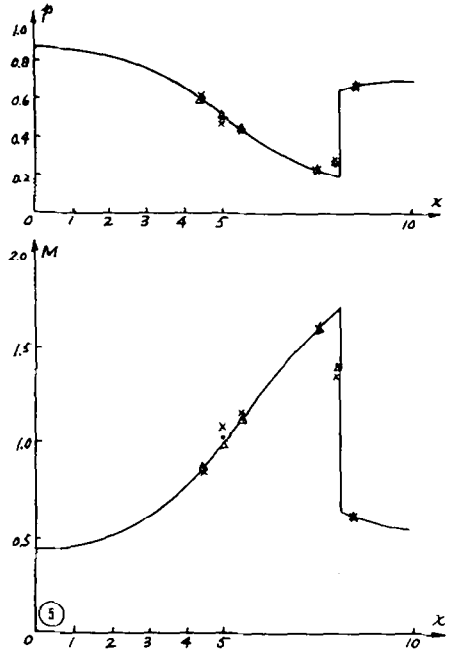

FIG. 5. Nozzle $p_e = 0.70$. (—) Exact solution. (Δ) Fixed b.c., $\Delta x = 0.5$, $q = 0.5$, $n = 592$, $\varepsilon = 0.8 \times 10^{-4}$; $n = 896$, $\varepsilon = 0.6 \times 10^{-6}$ ($m_0 = 0.9155$). (×) Lengthen the duct b.c., $\Delta x = 0.5$, $q = 0.5$, $n = 928$, $\varepsilon = 0.4 \times 10^{-4}$; $n = 1536$, $\varepsilon = 0.1 \times 10^{-5}$ ($m_0 = 0.9109$). (·) Scheme b.c., $\Delta x = 0.5$, $q = 0.5$, $n = 480$, $\varepsilon = 0.9 \times 10^{-4}$ ($m_0 = 0.916$); $q = 0.7$, $n = 352$, $\varepsilon = 0.8 \times 10^{-4}$ ($m_0 = 0.916$).

In the following, only numerical results with this type of boundary conditions and with $\Delta x = 0.5$, $\varepsilon \doteq 10^{-4}$, will be discussed.

We mention that in the case of $p_e = 0.70$, if $q = 0.82$ (which is about the stability limit), then $n \sim 304$. If $q_j = 1/(\lambda_+)_j$ then $n \sim 256$; that is, with variable Δt such that the Courant number is equal to one, the convergence is faster, which agrees with the analysis in [8].

We also mention here that the MacCormack scheme is not stable for $p_e = 0.70$.

To test the upwind scheme further for different shock positions, eight other cases, with $p_e = 0.72, 0.74, \ldots, 0.86$, were computed. For each case there was at most one point of transition, see Figs. 6–14, where only the result at the point of transition is shown by ·. But the point of transition itself is determined by $u_{j_M - 1/2}$ being supersonic and $u_{j_M + 1/2}$ being subsonic, and expression (5.1), when involving M, cannot always represent the value of u midway between the mesh points, see Figs. 7, 12; note $m_M < m_0$ in this situation. Changing to

$$u_{j+1/2} = \frac{1}{2}\left[\frac{(\rho u S)_j}{(\rho S)_j} + \frac{(\rho u S)_{j+1}}{(\rho S)_{j+1}}\right] \tag{5.2}$$

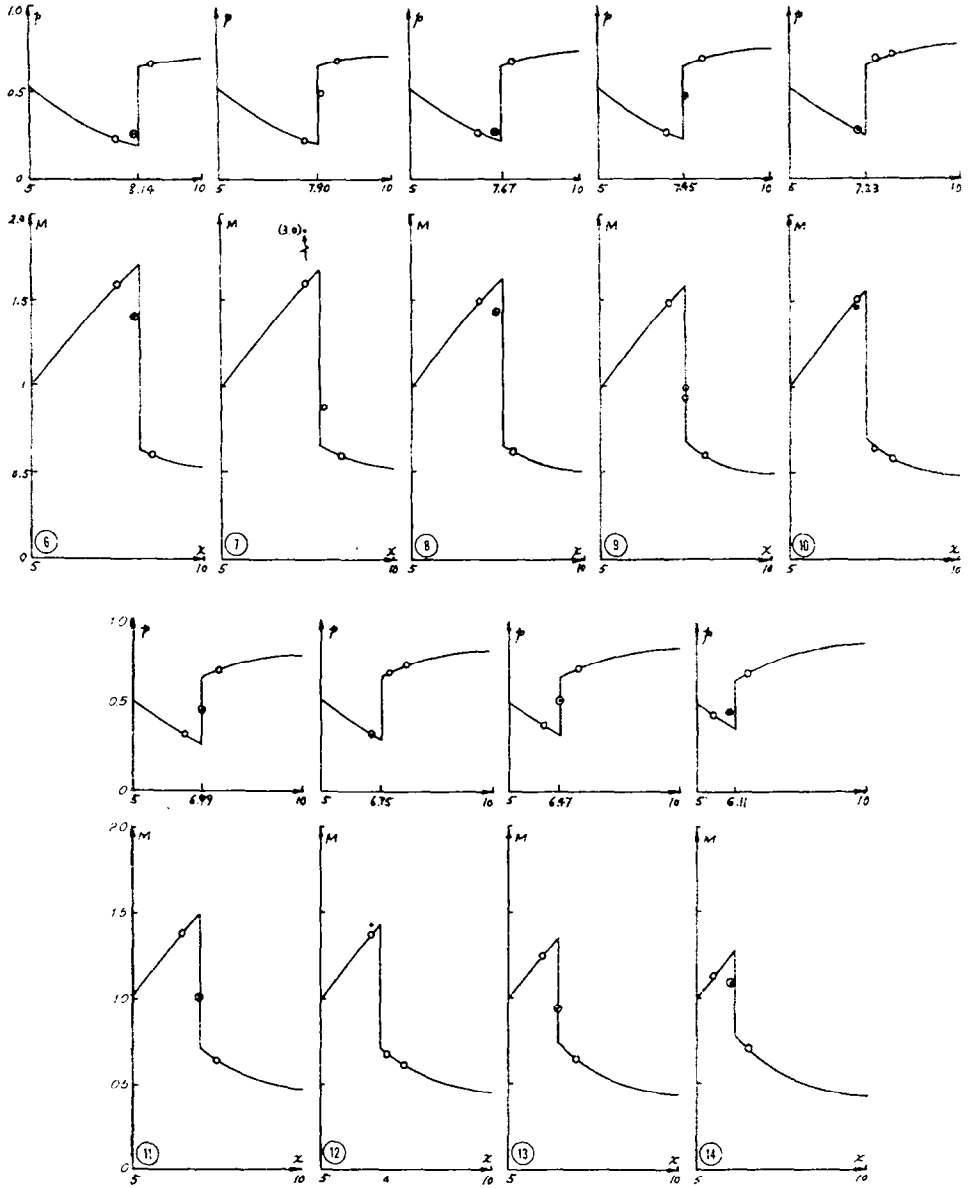

FIGS. 6–14. (6) Nozzle $p_e = 0.70$ ($m_0 = 0.9158$, $m_M = 0.9541$). (7) Nozzle $p_e = 0.72$ ($m_0 = 0.9157$, $m_M = 0.9788$). (8) Nozzle $p_e = 0.74$ ($m_0 = 0.9158$, $m_M = 0.9386$). (9) Nozzle $p_e = 0.76$ ($m_0 = 0.9159$, $m_M = 0.9730$). (10) Nozzle $p_e = 0.78$ ($m_0 = 0.9134$, $m_M = 0.9099$). (11) Nozzle $p_e = 0.80$ ($m_0 = 0.9159$, $m_M = 0.9607$). (12) Nozzle $p_e = 0.82$ ($m_0 = 0.9156$, $m_M = 0.9212$). (13) Nozzle $p_e = 0.84$ ($m_0 = 0.9150$, $m_M = 0.9446$). (14) Nozzle $p_e = 0.86$ ($m_0 = 0.9140$, $m_M = 0.9278$).

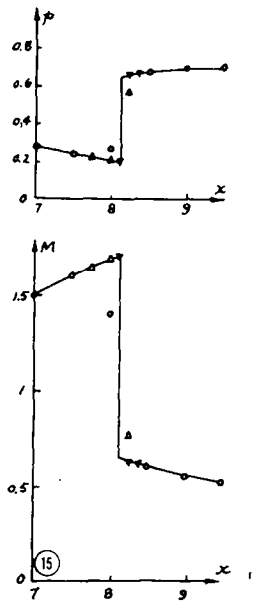

FIG. 15. Nozzle $p_e = 0.70$ sharpening the shock. (○) original mesh, $\Delta x = 0.5$, $q = 0.7$, $n = 352$, (△) $\Delta x = 0.25$, $n \to 652$. (▼) $\Delta x = 0.125$, $n \to 652 + 960$.

improved matters; the results at L, M, and R are shown in Figs. 6–14 by ○. Other than $p_e = 0.78$, Fig. 10 (the result in this case is really not bad), the values at M are between those at L and R, the shock position is within half a mesh width of M, and $m_M > m_0$. If the shock position is exactly halfway between two neighboring mesh points, then there is no transition point, the case of 0.82, Fig. 12, is close to this.

For the profile of the numerical shock to be even sharper, the mesh can be refined near the shock, and iteration continued locally; that is, after obtaining results on the original mesh, divide the LR interval into four equal parts, the results at the original L and R are taken as fixed boundary values on the new I and E points, then the computation is continued on the 5 point interval until steady state is reached again. This process can be repeated until the shock profile has the desired sharpness. This procedure was tested for $p_e = 0.70$, 0.78, 0.86, twice halving the mesh size. The results for $p_e = 0.70$ are shown in Fig. 15 (note the scale on the horizontal axis has been doubled). The computations for the other two cases were also successful.

6. The Implicit Upwind Scheme

To improve the rate of convergence, we will consider the implicit upwind scheme in this section. For (3.1) the implicit upwind scheme is

$$u_j^{n+1} + r(u_j^{n+1} - u_{j-1}^{n+1}) = u_j^n, \tag{6.1}$$

we have

$$\alpha_I = \frac{1}{1+r}. \tag{6.2}$$

We see that the larger r is, the higher the asymptotic rate of convergence. Similar to the explicit case, (6.1) can be written as a full implicit center-space difference scheme with a certain viscosity term. From [8], we know that with this scheme, for larger r, $\|C_\Delta^n\|_1$ decreases as n increases from the very beginning, which is a desirable property for an iterative scheme to have. For our problem, we have, corresponding to (3.12), the scheme

$$\begin{aligned} U_j^{n+1} &+ \frac{q}{2}\left[(F_{j+1}^{n+1} - F_{j-1}^{n+1}) + S_{j+1/2}(G_{j+1}^{n+1} - G_j^{n+1}) + S_{j-1/2}(G_j^{n+1} - G_{j-1}^{n+1})\right] \\ &- \frac{q}{2}\{\operatorname{sign} C_{j-1/2}^n[(F_{j+1}^{n+1} - F_j^{n+1}) + S_{j+1/2}(G_{j+1}^{n+1} - G_j^{n+1})] \\ &- \operatorname{sign} C_{j-1/2}^n[(F_j^{n+1} - F_{j-1}^{n+1}) + S_{j-1/2}(G_j^{n+1} - G_{j-1}^{n+1})]\} = U_j^n, \end{aligned} \tag{6.3}$$

where for the sake of convenience, sign C is taken on the nth level. Simplifying (6.3) as in [10], we obtain from (2.8), (2.9),

$$F^{n+1} \sim F^n + \left(\frac{\partial F}{\partial U}\right)^n (U^{n+1} - U^n) = F^n + A^n(U^{n+1} - U^n) = A^n U^{n+1},$$

$$G^{n+1} \sim G^n + \left(\frac{\partial G}{\partial U}\right)^n (U^{n+1} - U^n) = G^n + B^n(U^{n+1} - U^n) = B^n U^{n+1}.$$

By substituting into (6.3) and rearranging we arrive at

$$\begin{aligned} &-\frac{q}{2}(I + \operatorname{sign} C_{j-1/2}^n)(A_{j-1}^n + S_{j-1/2}B_{j-1}^n)\, U_{j-1}^{n+1} \\ &+ \left[I + \frac{q}{2}(I + \operatorname{sign} C_{j-1/2}^n)(A_j^n + S_{j-1/2}B_j^n)\right. \\ &\left. + \frac{q}{2}(-I + \operatorname{sign} C_{j+1/2}^n)(A_j^n + S_{j-1/2}B^n)\right] U_j^{n+1} \\ &+ \frac{q}{2}(I - \operatorname{sign} C_{j+1/2}^n)(A_{j+1}^n + S_{j+1/2}B_{j+1}^n)\, U_{j+1}^{n+1} = U_j^n. \end{aligned} \tag{6.4}$$

With scheme boundary conditions (all coefficients involving values to the left/right of the left/right boundary are zero), (6.4) forms a system of linear algebraic equations with a block tridiagonal matrix and hence can be easily solved.

With difference scheme (6.4), where $q = 16$, three cases of the nozzle example, $p_e = 0.70$, 0.78, and 0.86, were computed. For $p_e = 0.70$, results with $m_0 = 0.9155$, $m_M = 0.9542$ were obtained; for $p_e = 0.78$, $m_0 = m_M = 0.9159$; and for $p_e = 0.86$, $m_0 = 0.9132$, $m_M = 0.9274$. The results plotted on graph are about the same as those obtained with the explicit upwind scheme (i.e., Figs. 6, 10, and 14).

Also $q = 32$ and 64 were tried for the case $p_e = 0.70$. With $q = 64$ instability occurred; we would expect some limitation on the time step size because of sign C^n. With $q = 32$, the number of iterations $n = 24$, which is a lot less than that with the explicit upwind scheme, but the work per level with the implicit scheme is a lot more. On the FELIX C-512 computer, the explicit upwind scheme with $q = 0.82$ took about 10 sec, while the implicit upwind scheme with $q = 32$ took about 4 sec. So we can save more than half the computing time with the implicit upwind scheme.

We point out in passing, that the leapfrog–Dufort–Frankel scheme was also tested, but the work per point was a lot more than that of the explicit upwind scheme, so that the total amount of work per problem increased. Hence we do not discuss this scheme here.

7. Concluding Remarks

This paper presents unsteady schemes (or iterative schemes) for steady-state one-dimensional discontinuous solutions starting from the pseudo-unsteady equation. The so-called explicit upwind scheme is actually an explicit forward-time, center-space difference scheme with an appropriate artificial viscosity term. Using the matrix properties of the pseudo-unsteady equation, a sign C depending on the directions of the characteristics in the viscosity term is defined; the stability of the scheme, as a scheme for pure initial value problems, and the convergence of the scheme, as an iterative scheme with appropriate boundary conditions, can be easily analyzed. With the scheme boundary conditions, the numerical method consists of embedding a steady-state first order difference problem (for smooth solution, (3.14a)) into an unsteady, (or pseudo-unsteady) second order (in space) difference problem. The viscosity term has an effect in the unsteady process—it speeds up convergence; it has an effect in the steady state only in the shock region—it yields numerical shocks with at most one point of transition, but it does not influence the solution in the smooth region, as seen from (3.14), (3.16). A series of numerical experiments with different shock positions demonstrates that this is indeed so. The mesh can be refined locally and computation continued locally to make the profile of a discontinuous solution sharper. To increase the rate of iterative convergence, the implicit upwind scheme can be used, more than half of the amount of work can be saved.

Whether the one-dimensional schemes presented can be extended successfully to more complicated and two-dimensional problems will be investigated.

REFERENCES

1. L. CROCCO, *AIAA J.* **3** (1965), 1824–1832.
2. A. J. CHORIN, *J. Comput. Phys.* **2** (1967), 12–26.
3. J. D. DENTON, "A Time Marching Method for Two- and Three-Dimensional Blade to Blade Flows," ARC R&M No. 3775, 1975.
4. A. J. CHORIN, *J. Comput. Phys.* **22** (1976), 517–533.
5. B. ENGQUIST AND S. OSHER, *Math. Comput.* **34** (1980), 45–75.
6. R. W. MACCORMACK, A. W. RIZZI, AND M. INOUYE, *in* „Computational Methods and Problems in Aeronautical Fluid Dynamics," Academic Press, New York London, 1976.
7. P. J. ROACHE, "Computational Fluid Dynamics," Hermosa Publishers, Albuquerque, N. Mex., 1972
8. L. C. HUANG, *J. Numer. Methods Comput. Appl.*, in press. [In Chinese.]
9. Y. K. ZHANG, M. Y. SHEN, AND Z. J. GONG, *Math. Numericae Sinica* **4** (1978), 9–26. [In Chinese.]
10. R. M. BEAM AND R. F. WARMING, *J. Comput. Phys.* **22** (1976), 87–110.
11. J. L. STEGER, *Comput. Methods Appl. Mech. Eng.* **13** (1978), 175–188.
12. R. F. WARMING, R. M. BEAM, AND B. J. HYETT, *Math. Comput.* **29** (1975), 1037–1045.
13. H. LOMAX AND J. L. STEGER, *Annu. Rev. Fluid Mechn.* **7** (1975), 63–88.
14. J. A. TORRES AND R. C. BAKER, *Comput. Fluids* **7** (1979), 177–190.
15. M. J. ZUCROW AND J. D. HOFFMAN, "Gas Dynmaics," Vol. I, Wiley, New York, 1976.